MEASUREMENT OF SIX DEGREE OF FREEDOM MODEL MOTIONS USING STRAPDOWN ACCELEROMETERS

M.D. Miles

Hydraulics Laboratory
National Research Council
Ottawa, Canada

ABSTRACT

A method for the measurement of ship model motions in oblique seas using seven strapdown accelerometers is described which provides a light, reliable and inexpensive alternative to other systems such as gyro-stabilized platforms or optical tracking devices. Although linearized analysis is satisfactory for roll, pitch and heave motions at angles up to 15 degrees, significant errors can occur in yaw, surge and sway displacements at roll and pitch angles as low as 5 degrees due to residual gravity terms, nonlinear cross-coupling and convolution of energy to lower frequencies.

An alternative iterative analysis procedure is described which uses an FFT-based integration technique to solve the full nonlinear differential equations for the displacement motions. The average roll and pitch angles are also determined by resolving the mean direction of the gravity field. Numerical simulations using typical motion spectra have shown that the nonlinear procedure converges at angular motions up to 60 degrees and reduces errors by an order of magnitude compared to linearized analysis. Model test results for a prototype of the strapdown system are also presented.

1.0 INTRODUCTION

A variety of methods have been used in ship model basins to measure vessel motions during seakeeping tests. These include instrumented linkages to carriages, angular position and rate gyros, fixed and gyro-stabilized accelerometers, ultrasonic ranging devices and, more recently, optical tracking systems [1]. Since the NRC seakeeping basins are not equipped with carriages, inertial sensors have generally been preferred and gyro-stabilized platforms have been used extensively for both model tests and full scale trials. Although gyro systems provide sufficient accuracy, their initial cost is fairly high and they also tend to require frequent and expensive maintenance. Their relatively high weight and power requirements also preclude their use in smaller radio-controlled models.

Gyro-stabilized platforms have also been widely used in inertial navigation systems for aircraft but are now being superseded by strapdown systems which have become practical with the advent of microprocessors and improved sensor technology to cope with the wider dynamic range requirements. The strapdown systems employ rate gyros and accelerometers which are fixed to the vehicle frame and offer advantages of increased reliability and lower cost, weight and power consumption compared to gimballed systems.

A system of 3 fixed accelerometers had previously been used at NRC to measure heave, pitch and surge in regular head seas with performance comparable to that of a gyro platform. It was therefore decided to develop a strapdown system to measure oscillatory motion in 6 degrees of freedom in irregular waves. Although ring laser gyros provide a technically attractive alternative to mechanical rate gyros for strapdown systems, currently available models were found to be prohibitively expensive. Since this application is less demanding than inertial navigation, it was decided to eliminate the rate gyros and use only accelerometers. This approach requires an additional level of integration for the angular motions but allows the use of more reliable and less expensive instrumentation.

Although 6 accelerometers are sufficient to measure 6 degree of freedom motion, it was decided to use 7 instead so that they could all be located in one plane in order to simplify installation and to minimize the effect on the vertical mass distribution of the model. The proposed system was first evaluated by computer simulation and model tests were subsequently carried out on a prototype unit with an optical tracking system for comparison.

2.0 EQUATIONS OF MOTION

In order to utilize a strapdown system, it is first necessary to derive equations of motion which define the fundamental motions of the rigid body in terms of the measured accelerations. Consider a vessel oscillating in 6 degrees of freedom about an equilibrium position which moves at constant velocity relative to the earth. Acceleration effects due to earth rotation, such as Coriolis force, may be neglected in this application. Using standard ITTC and SNAME [2] notation, let (x_0, y_0, z_0) denote an inertial frame which moves relative to the earth at the average velocity of the vessel. The z_0 axis is vertically downwards and the x_0 axis is aligned with the average heading of the vessel. Let (x,y,z) denote the body axes of the vessel. The 7 accelerometers are mounted in the x-y plane as shown in Fig. 1 where C is an arbitrary reference point. Accelerometers 1,2,5 & 6 are sensitive in the z direction, 3 & 4 are sensitive in the y direction and 7 is sensitive in the x direction. Let $\vec{x}_0(Q)$ be the vector to some arbitrary point Q on the vessel and let $\vec{x}(CQ)$ be the vector from C to Q. Since $\vec{x}(CQ)$ is constant,

$$\ddot{\vec{x}}_0(Q) = \ddot{\vec{x}}_0(C) + \ddot{A}\,\vec{x}(CQ) \qquad (1)$$

where A is the rotation matrix given by

$$\begin{pmatrix} \cos\theta\cos\psi & \sin\theta\sin\phi\cos\psi - \cos\phi\sin\psi & \sin\theta\cos\phi\cos\psi + \sin\phi\sin\psi \\ \cos\theta\sin\psi & \sin\theta\sin\phi\sin\psi + \cos\phi\cos\psi & \sin\theta\cos\phi\sin\psi - \sin\phi\cos\psi \\ -\sin\theta & \cos\theta\sin\phi & \cos\theta\cos\phi \end{pmatrix}$$

Applying (1) at each accelerometer location and taking the dot product with the unit vector of the sensitive axis, it follows that

$$\ddot{\vec{x}}_0(C) = A\,\vec{P} + g\hat{k}_0 \qquad (2)$$

where

$\hat{k}_0$ = unit vector in the z_0 direction,

$P_1(t) = a_7$,

$P_2(t) = (R_4 a_3 + R_3 a_4)/(R_3 + R_4)$,

$P_3(t) = (R_2 a_1 + R_1 a_2)/(R_1 + R_2)$,

a_j = acceleration measured by accelerometer j and

R_j = the radial distance from point C to accelerometer j.

Equation 2 gives the translatory acceleration at point C in terms of the measured vector $\vec{P}$ and the rotation matrix A. Once A has been determined as a function of time, each component of (2) can be integrated separately to obtain the surge, sway and heave velocities and displacements.

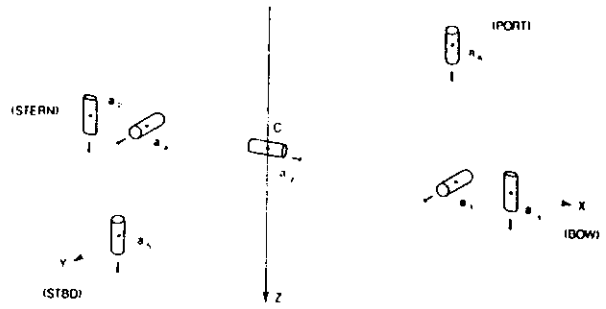

FIGURE 1 CONFIGURATION OF STRAPDOWN ACCELEROMETERS

The angular accelerations are obtained by subtracting the signals from each pair of accelerometers. For example, applying (1) at accelerometers 5 and 6,

$$a_5 = \hat{k}\cdot[A^{-1}\,(\ddot{\vec{x}}_0(C) - g\hat{k}_0)] + R_5\hat{k}\cdot[A^{-1}\,\ddot{A}\,\hat{j}] \qquad (3)$$

and $a_6 = \hat{k}\cdot[A^{-1}\,(\ddot{\vec{x}}_0(C) - g\hat{k}_0)] - R_6\hat{k}\cdot[A^{-1}\,\ddot{A}\,\hat{j}] \qquad (4)$

where $\hat{i},\hat{j},\hat{k}$ are unit vectors in the x,y,z directions.

Let $F_1(t) = (a_5 - a_6)/(R_5 + R_6)$.

$$\therefore\quad F_1 = \hat{k}\cdot[A^{-1}\,\ddot{A}\,\hat{j}]\ . \qquad (5)$$

It is shown in ref. 3 that

$$\dot{A} = A\,\Omega \qquad (6)$$

where $\Omega = \begin{pmatrix} 0 & -\omega_z & \omega_y \\ \omega_z & 0 & -\omega_x \\ -\omega_y & \omega_x & 0 \end{pmatrix}$

and ω_x, ω_y and ω_z are the components of the angular velocity vector resolved along the body axes. It can be shown, by considering the small angle rotations which occur over a time interval Δt, that these are related to the SNAME Euler angles as follows:

$$\omega_x = \dot{\phi} - \dot{\psi}\sin\theta$$

$$\omega_y = \dot{\theta}\cos\phi + \dot{\psi}\cos\theta\sin\phi \qquad (7)$$

$$\omega_z = -\dot{\theta}\sin\phi + \dot{\psi}\cos\theta\cos\phi$$

It follows from (6) that $\ddot{A} = A\,B$ where $B = \Omega^2 + \dot{\Omega}$ and hence $F_1 = B_{32}$. Defining similar functions for the other accelerometers, we obtain

$$\dot{\omega}_x = F_1(t) - \omega_y \omega_z \qquad (8)$$

$$\dot{\omega}_y = F_2(t) + \omega_x \omega_z \qquad (9)$$

and $$\dot{\omega}_z = F_3(t) - \omega_x \omega_y \qquad (10)$$

where $F_2(t) = (a_2 - a_1)/(R_1 + R_2)$

and $F_3(t) = (a_3 - a_4)/(R_3 + R_4)$.

Equations 8-10 are the fundamental relations defining the rotation rates in terms of the measured quantities F_1, F_2 and F_3. The Euler angles are then defined by

$$\dot{\phi} = \omega_x + \tan\theta\ (\omega_y \sin\phi + \omega_z \cos\phi) \qquad (11)$$

$$\dot{\theta} = \omega_y \cos\phi - \omega_z \sin\phi \qquad (12)$$

$$\dot{\psi} = (\omega_y \sin\phi + \omega_z \cos\phi)/\cos\theta \qquad (13)$$

which follow from (7).

Equations 8-10 must first be solved numerically to obtain ω_x, ω_y and ω_z. Equations 11 and 12 are then solved for ϕ and θ and ψ is obtained by integrating (13). The rotation matrix is then defined so (2) can be integrated to obtain surge, sway and heave.

3.0 ANALYSIS PROCEDURE

If the motions are sufficiently small, the linearized form of the equations can be used. In this case, $\ddot{\phi} = F_1(t)$, $\ddot{\theta} = F_2(t)$ and $\ddot{\psi} = F_3(t)$ so the angular motions are obtained by direct numerical integration. Similarly, $\ddot{x}_0(C) = P_1(t) - g\theta$, $\ddot{y}_0(C) = P_2(t) + g\phi$ and $\ddot{z}_0(t) = P_3(t) + g$ so surge, sway and heave are also obtained by double integration. The linearized equations are not sufficiently accurate for most practical applications, however.

The following iterative technique was found to be very effective in solving the full nonlinear equations of motion. Initial estimates of the average roll and pitch angles are first computed from

$$\phi_0 = -\overline{P_2(t)}/g \quad \text{and} \quad \theta_0 = \overline{P_1(t)}/g$$

which follow from imposing the condition of zero average surge and sway acceleration on the linearized form of (2). The angular velocities are then computed using the following iteration equations:

$$\dot{\omega}_x(n+1,t) = F_1(t) - \omega_y(n,t) * \omega_z(n,t)$$

$$\dot{\omega}_y(n+1,t) = F_2(t) + \omega_x(n,t) * \omega_z(n,t)$$

$$\dot{\omega}_z(n+1,t) = F_3(t) - \omega_x(n,t) * \omega_y(n,t)$$

An FFT-based integration routine incorporating a high pass filter is used at each step of the iteration process. The filter cut-off point, FC, is selected to prevent excessive amplification of low frequency noise. The integration constants are obtained by imposing the condition that the average angular velocities are zero for oscillatory motion. After the ω's have been computed, the following iteration equations are used to calculate roll and pitch:

$$\dot{\phi}(n+1,t) = \omega_x + \tan(\theta(n,t)) * (\omega_y \sin\phi(n,t) + \omega_z \cos\phi(n,t))$$

$$\dot{\theta}(n+1,t) = \omega_y \cos\phi(n,t) - \omega_z \sin\phi(n,t)$$

Yaw is then computed by direct integration of (13) and final estimates of the average roll and pitch angles are obtained by adding constant perturbations to satisfy the condition that the average surge and sway accelerations from (2) are zero. The average roll and pitch angles are thus determined by measuring the mean direction of the gravity vector relative to the vessel frame. Finally, surge, sway and heave at any arbitrary point Q are obtained by integrating each component of

$$\ddot{\vec{x}}_0(Q) = A\,[\vec{P} + B\,\vec{x}(CQ)] + g\hat{k}_0 \qquad (14)$$

which follows from (1) and (2).

4.0 NUMERICAL SIMULATION

Two different methods were used to synthesize signals for the numerical simulations which were used to evaluate the proposed system. In the first method, time series for each degree of freedom were synthesized using a random phase method such that all motions had the same spectral shape but the time series were uncorrelated. The linear and nonlinear analysis procedures were then used to estimate the fundamental motions from the synthesized accelerometer signals. The simulation results were compared mainly on the basis of the Normalized RMS Error or NRE which is defined as follows:

$$NRE = 100 * RMS[X1(t)-X2(t)]/(4*RMS[X2(t)])\ \%$$

where X1(t) is the motion estimated from the accelerometer signals and X2(t) is the actual motion. The NRE was calculated for accelerations, velocities and displacements but the largest errors usually occurred in displacements.

The relative performance of the linear and nonlinear analysis procedures for angular motions is shown in Fig. 2. The nonlinear iterative procedure is far superior with NRE's of less than 2 percent for simultaneous roll, pitch and yaw motions up to 15

degrees rms (45 degrees peak). The NRE's of the linear procedure are an order of magnitude larger and it would not be useful at amplitudes much above 3 degrees rms. It should be noted, however, that the linear procedure will work better in planar motion cases where one angle dominates because the product terms in equations 8-10 are then small.

The linear procedure also has poor low frequency performance, even at fairly small amplitudes, as shown in Fig. 3. In this case, the actual motion spectra do not contain any significant energy at frequencies below 0.25 Hz. As the analysis cut-off frequency is reduced below this point, the nonlinear procedure errors stabilize at small values whereas the linear procedure errors grow rapidly. These errors are caused by low frequency components in F_1, F_2 and F_3 due to convolution of the roll, pitch and yaw spectra by the nonlinear centripetal acceleration terms. This appears as low frequency noise to the linear procedure which is amplified by integration.

In the second simulation method, an irregular encountered wave train was first synthesized and the time series for the fundamental motions were then computed using strip theory transfer functions. This method produced more realistic correlated ship motions with proper relative phasing. The simulations were done using a frigate hull form and a typical result using the iterative procedure is shown in Fig. 4. The NRE's for all motions are less than 2 percent for H_S up to 15 m which produced peak roll and pitch angles of 30 degrees and 12 degrees respectively.

The NRE is also significantly smaller for roll, pitch and heave than for surge, and sway. This effect showed up in all simulations and is caused mainly by the fact that the vertical accelerometers are weakly coupled to the gravity field through the cosines of roll and pitch. Consequently, roll and pitch errors have a much smaller effect on heave than on surge and sway which are strongly coupled to gravity by the sines of roll and pitch. Roll and pitch must therefore be measured very accurately for good surge and sway results since a 1 percent roll error can easily generate a 10 percent sway error.

The range of convergence of the iterative procedure was also checked by simulation. In both the correlated and uncorrelated motion cases, the procedure never failed to converge until the peak angles exceeded 60 degrees, which should be adequate for most seakeeping work with the exception of extreme situations such as capsizing. The procedure normally converges in about 6 iterations at peak angles up to 20 degrees but 30 to 40 iterations may be required at larger angles.

The effect of measurement noise was investigated by adding Gaussian white noise to each of the synthesized accelerometer signals. As shown in Fig. 5, rms measurement noise up to 2 percent is tolerable for roll, pitch and heave but it must be kept below 0.2 percent for good surge, sway and yaw accuracy.

Since the analysis procedure uses an FFT integrator, the number of points in each time series must be a power of 2 and all signals must be cyclic. The first condition is easily satisfied by resampling at a smaller time step using simple parabolic interpolation. The measured signals must also be forced to be cyclic in order to prevent large surge and sway errors which otherwise result from Gibbs phenomenon. Tapering the signals to zero at each end greatly reduces these errors but a technique called cyclic merging was found to be more effective as shown in Fig. 6. This consists of overlapping the tapered zones to form a continuous cyclic splice without reducing signal amplitude. The effect of cyclic merge length is shown in Fig. 7. A merge length of 5 percent is usually satisfactory so the original record length will normally be reduced by about 10 percent during analysis. Cyclic merging is not necessary in regular waves since a cyclic segment can be selected for processing.

As noted previously, it is necessary to use a low frequency cut-off, FC, during the integration process. The effect of this parameter was also investigated by simulation and a typical result is shown in Fig. 8. The choice of FC is not critical for roll, pitch, yaw and heave but low frequency surge and sway errors will result if FC is set too low. The optimum value for FC is generally about 0.8*f1 where f1 is defined as the frequency such that 99 percent of the energy of the encountered wave spectrum lies above f1.

5.0 MODEL TESTS

A prototype strapdown accelerometer system was built and tested on 1:40 scale models of an offshore supply vessel and a semisubmersible platform. The models were tested in both regular and irregular waves in the Offshore Wave Basin of the NRC Hydraulics Laboratory. Sundstrand QA-1400 servo accelerometers were selected since they are specifically designed for inertial navigation applications having a resolution of 1 μg and a linearity error of less than 20 μg/g. They were mounted on a rigid aluminum frame with a roll separation of 30 cm, a pitch separation of 84 cm and a yaw separation of 95 cm.

An OPTOPOS optical tracking system [4] was used to make independent measurements of the model motions for comparison. This system uses 5 cameras to measure the (x,y,z) positions of 3 infra-red light emitting diodes (LED's) mounted on the model. The position of each LED is measured with a specified accuracy of about 1 mm and the 6 degree of freedom model motions are then computed geometrically by means of a software package supplied with the system.

A typical example of the roll, pitch and yaw motions measured by the two systems on the offshore supply vessel is shown in Fig. 9. The overall agreement is very good, even at roll angles up to 20 degrees. Localized differences, such as pitch and yaw at 57 seconds, were probably caused by occasional false readings in the OPTOPOS due to reflected light. In later tests on the semisubmersible, most of these false readings were eliminated by mounting the LED's higher on the model.

The accelerometer data were also used to compute surge, sway and heave at one of the LED positions for direct comparison with the raw OPTOPOS measurements. As shown in Fig. 10, the general agreement is quite good, especially in sway, but small differences tend to occur near the minima and maxima of the signals. Since this effect is indicative of undersampling, these differences are probably a consequence of the OPTOPOS sampling rate which had to be set at 5 Hz instead of the normal 10 Hz because of software constraints in the data acquisition system.

The roll, pitch and heave motions from one of the moored semisubmersible tests are shown in Fig. 11. In this case, the mooring lines were adjusted to produce average roll and pitch angles of -5 and +4 degrees. Roll and pitch agree very well and their mean values have also been accurately determined. Heave agreement is excellent in the lower frequency waves used in this test which supports the theory that the small differences observed at higher wave frequencies were caused mainly by the limited OPTOPOS sampling rate.

6.0 CONCLUSIONS

It has been demonstrated by numerical simulations and model tests that a strapdown system of 7 accelerometers can provide accurate acceleration, velocity and displacement measurements in 6 degrees of freedom for most types of seakeeping tests in both regular and irregular waves. The system has the advantages of high reliability, light weight, low power consumption and relatively low cost (approx. $15,000 U.S.).

The linearized analysis procedure is inadequate at peak angles above 10 degrees and at low frequencies. The nonlinear iterative analysis procedure was found to be much more accurate and can be used at peak angles up to 60 degrees. It also has better low frequency performance.

The most demanding motions for the strapdown system are surge and sway displacements and the accelerations must be measured very accurately in order to determine these motions with reasonable precision. This necessitates the use of inertial navigation grade accelerometers and a data acquisition system with at least 0.1 percent accuracy.

The strapdown system is not suitable for measuring surge and sway at very low frequencies. For example, it could not be used at low encounter frequencies in following seas or to measure moored platform surge due to second order long waves. A displacement measuring device, such as an optical tracking system, must be used in these situations. It should be noted that this is not a limitation of the strapdown approach per se, however, since any inertial system will have difficulties at very low frequencies.

Although optical tracking systems have excellent low frequency performance, velocities and accelerations computed from their displacement measurements tend to be somewhat noisy due to spatial resolution and sampling rate limitations. Thus, even when an optical system is available, it may be useful to supplement it with a strapdown accelerometer system for more accurate measurement of the higher frequency motions.

7.0 REFERENCES

(1) Report of the Seakeeping Committee, Section II.3, 15th ITTC, 1978.

(2) "Nomenclature for Treating the Motion of a Submerged Body Through a Fluid", SNAME T&R Bulletin 1-5, 1952.

(3) Britting, K.R., "Inertial Navigation System Analysis", Wiley-Interscience, 1971, pp. 11-17.

(4) Abelseth, L. and Rotvold, O., "A 3-Dimensional Position Measuring System", 16th ITTC, Vol. 1, 1981, pp. 507-516.

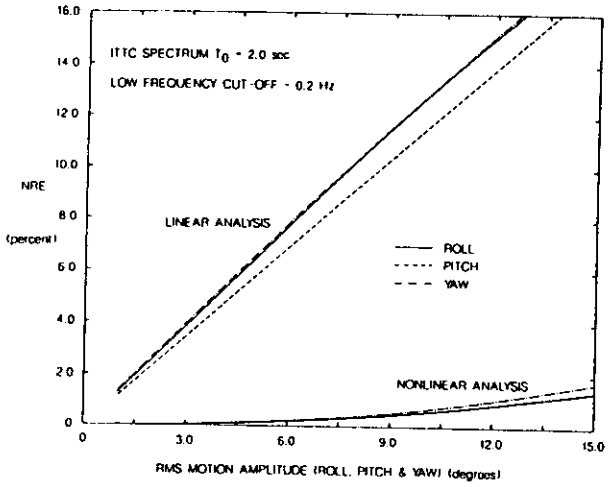

FIGURE 2 NORMALIZED RMS ERROR OF UNCORRELATED ROLL, PITCH AND YAW MOTIONS

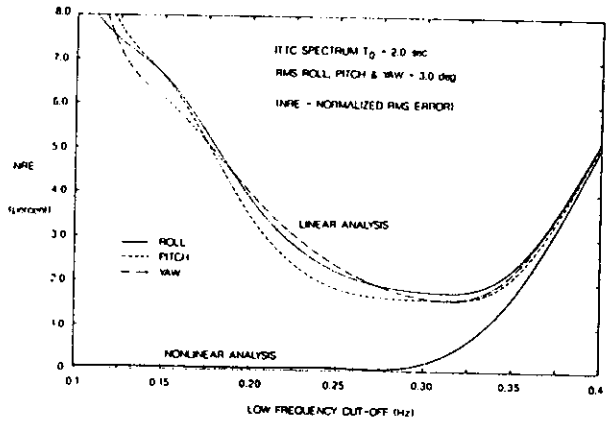

FIGURE 3 LOW FREQUENCY ROLL, PITCH AND YAW ERRORS

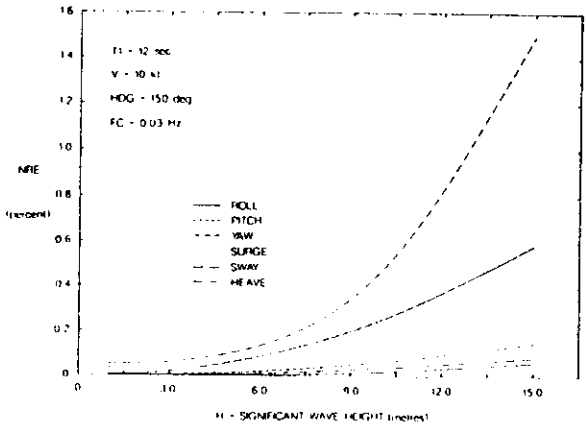

FIGURE 4 NONLINEAR ITERATIVE ANALYSIS OF SIMULATED FRIGATE MOTIONS

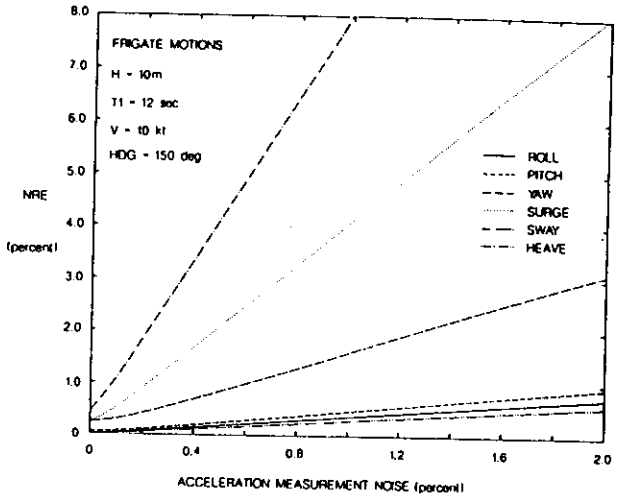

FIGURE 5 EFFECT OF MEASUREMENT NOISE ON COMPUTED DISPLACEMENTS

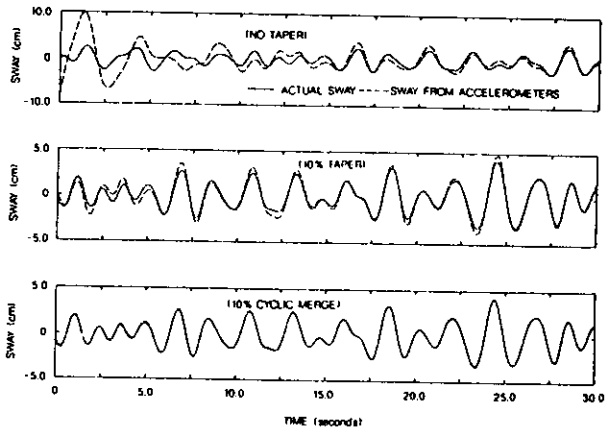

FIGURE 6 EFFECT OF TAPER AND CYCLIC MERGE ON FRIGATE SWAY MOTION (SCALE 1:40)

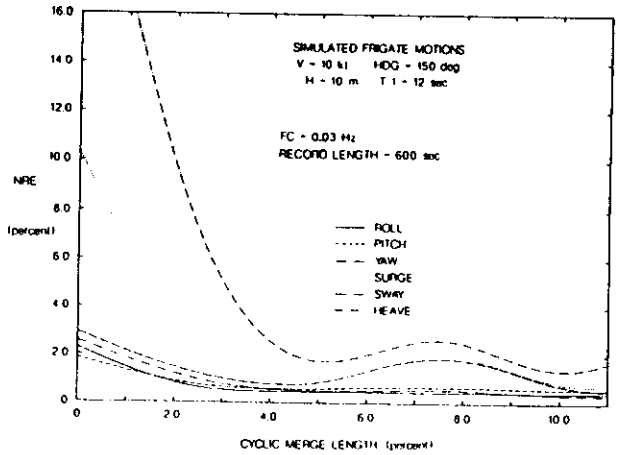

FIGURE 7 EFFECT OF CYCLIC MERGE LENGTH ON DISPLACEMENT ERRORS

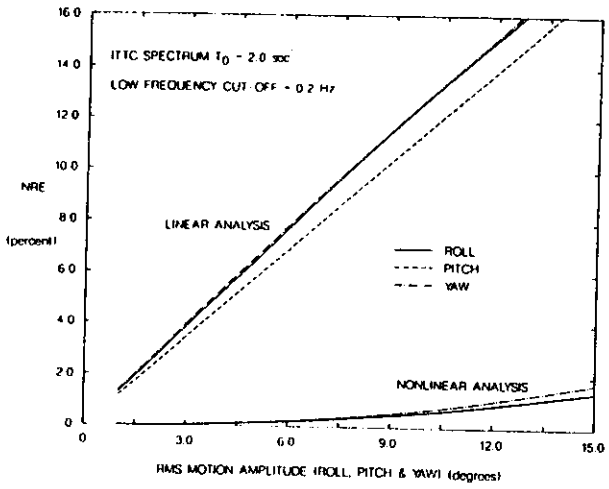

FIGURE 2 NORMALIZED RMS ERROR OF UNCORRELATED ROLL, PITCH AND YAW MOTIONS

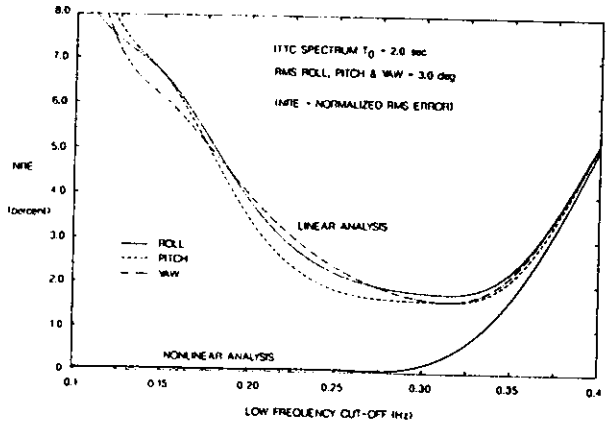

FIGURE 3 LOW FREQUENCY ROLL, PITCH AND YAW ERRORS

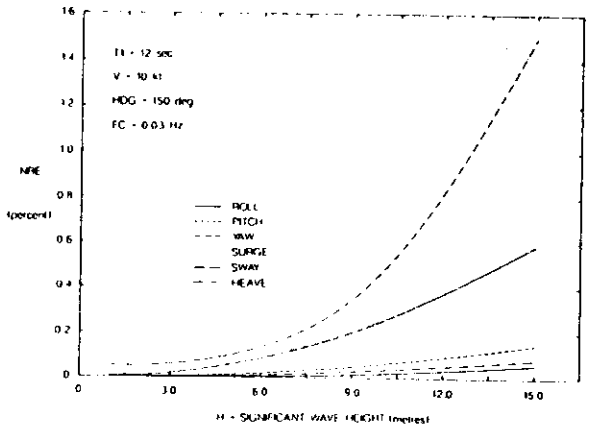

FIGURE 4 NONLINEAR ITERATIVE ANALYSIS OF SIMULATED FRIGATE MOTIONS

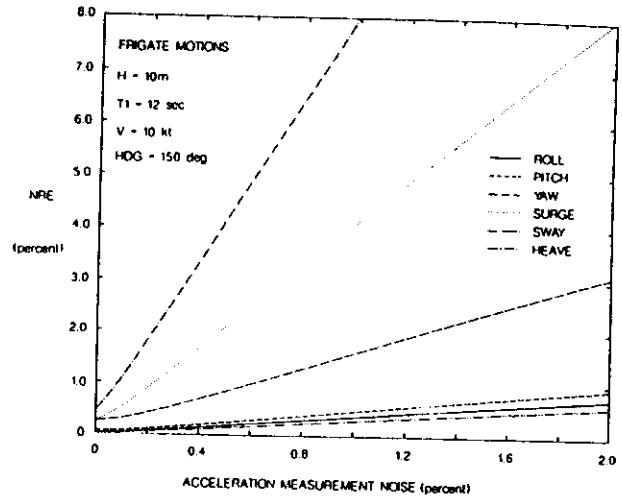

FIGURE 5 EFFECT OF MEASUREMENT NOISE ON COMPUTED DISPLACEMENTS

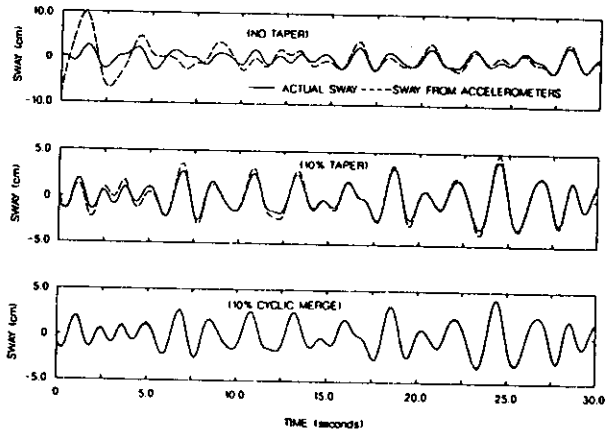

FIGURE 6 EFFECT OF TAPER AND CYCLIC MERGE ON FRIGATE SWAY MOTION (SCALE 1:40)

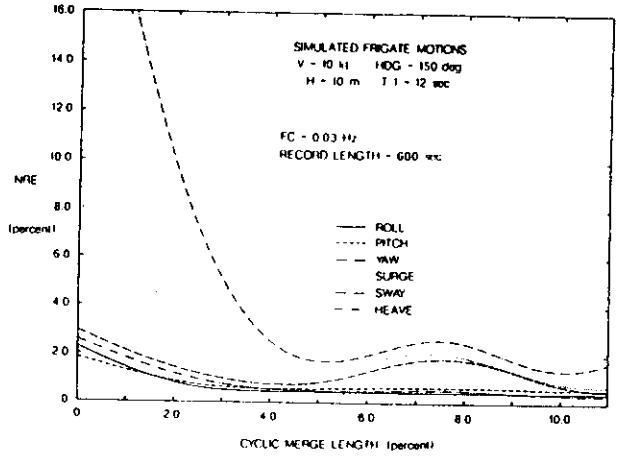

FIGURE 7 EFFECT OF CYCLIC MERGE LENGTH ON DISPLACEMENT ERRORS

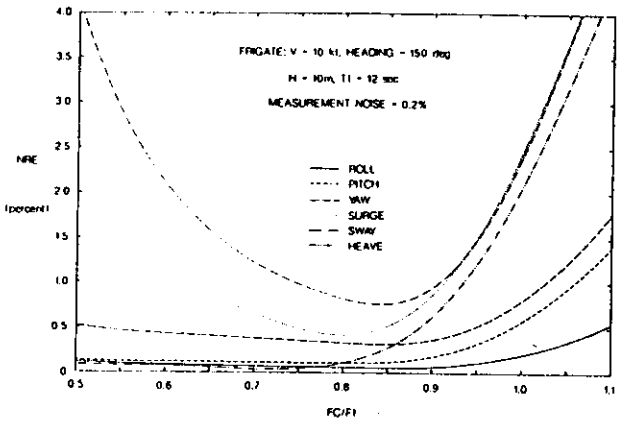

FIGURE 8 EFFECT OF CUT-OFF FREQUENCY FC ON DISPLACEMENT ERRORS

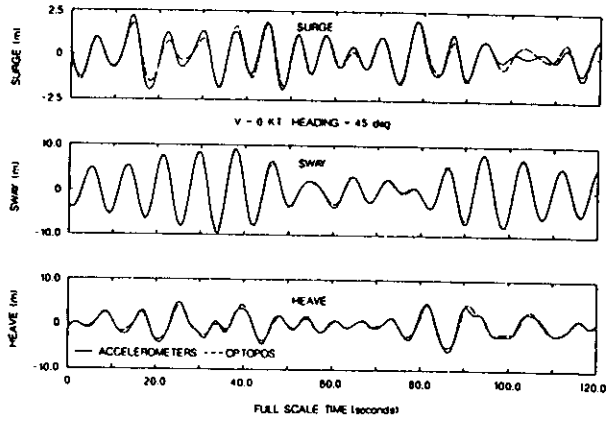

FIGURE 10 TRANSLATORY MOTION AT TRACKING LED NO.1 OF OFFSHORE SUPPLY VESSEL

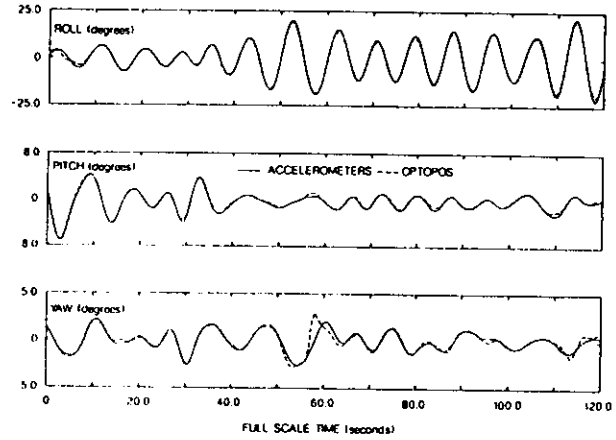

FIGURE 9 MODEL TEST OF OFFSHORE SUPPLY VESSEL-ROTATIONAL MOTIONS

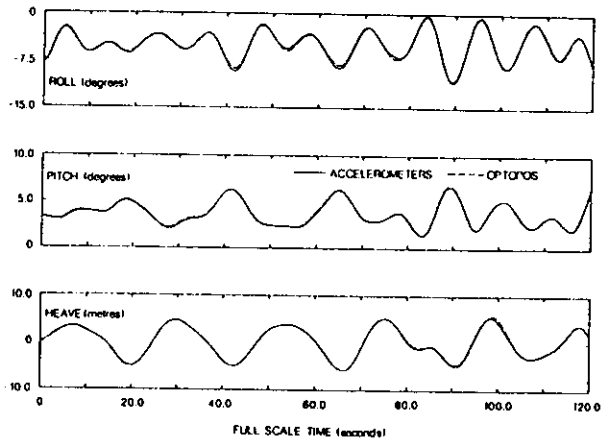

FIGURE 11 MODEL TEST OF MOORED SEMI-SUBMERSIBLE PLATFORM